Received October 15, 2018, accepted October 27, 2018, date of publication November 1, 2018, date of current version December 3, 2018.

Digital Object Identifier 10.1109/ACCESS.2018.2879160

A Fast Fluorescence Background Suppression Method for Raman Spectroscopy Based on Stepwise Spectral Reconstruction

SHUO CHEN[1], LINGMIN KONG[1], WENBIN XU[2], XIAOYU CUI[1], AND QUAN LIU[3]

[1]Sino-Dutch Biomedical and Information Engineering School, Northeastern University, Shenyang 110819, China
[2]Science and Technology on Optical Radiation Laboratory, Beijing 110854, China
[3]School of Chemical and Biomedical Engineering, Nanyang Technological University, Singapore 637457

Corresponding authors: Xiaoyu Cui (cuixy@bmie.neu.edu.cn) and Quan Liu (quanliu@ntu.edu.sg)

This work was supported in part by the National Natural Science Foundation of China under Grant 61605025 and Grant 61501101, in part by the Science and Technology Foundation of National Defense Key Laboratory under Grant 61424080209, in part by the Program for Innovation Talents in Universities of Liaoning Province under Grant LR2016031, in part by the Fundamental Research Funds for the Central Universities under Grant N171902001, in part by the Ministry of Education in Singapore under Grant MOE2015-T2-2-112, and in part by NTU-AIT-MUV Programme in advanced biomedical imaging under Grant NAM/15004.

ABSTRACT Raman spectroscopy is a rapid and non-destructive technique for detecting unique spectral fingerprints from biological samples. Raw Raman spectra often come with strong fluorescence background that makes spectral interpretation challenging. Although fluorescence background can be suppressed experimentally, this approach requires sophisticated and costly instruments. For convenience and cost-effectiveness, numerical methods have been used frequently to remove fluorescence background. Unfortunately, many of such methods suffer from long computation time. Therefore, a fast numerical method for fluorescence suppression is highly desirable especially in Raman spectroscopic imaging where Raman measurements from many pixels need to be processed rapidly. In response to this demand, we propose a fast numerical method for fluorescence background suppression based on the strategy of stepwise spectral reconstruction that we previously developed. Compared with traditional computational methods, including polynomial fitting, wavelet transform, Fourier transform, and peak detection, our results consistently show significant advantages in both accuracy and computational efficiency when tested on Raman spectra measured from phantoms and cells as well as surfaced enhanced Raman spectra from blood serum samples. In particular, our method yields clean Raman spectra closest to the reference results generated by polynomial fitting while several orders of magnitude faster than others. Therefore, the proposed fast fluorescence suppression method is promising in Raman spectroscopic imaging or related application in which high-computation efficiency is critical and a calibration dataset is available.

INDEX TERMS Biomedical signal processing, Raman spectroscopy, fluorescence suppression, Raman imaging.

I. INTRODUCTION

Raman spectroscopy is a powerful technique for analyzing bio-molecular structure and composition of biological samples based on the detection of vibrational, rotational and other low-frequency information about molecules [1], [2]. As Raman measurements can be carried out rapidly and non-destructively with minimal sample preparation, Raman spectroscopy has shown great potential in biomedical applications [3], [4], such as cell classification, cancer diagnosis and dentistry. However, the intrinsic fluorescence of biological samples forms strong background on which the Raman signal is superimposed, which makes the weak Raman signal difficult to be distinguished and post-processed [5], [6]. The presence of fluorescence background severely restricts the usage of Raman techniques in biomedical applications. Therefore, it is necessary to suppress fluorescence background before a Raman spectrum is further analyzed.

Over the past few decades, various approaches have been developed to suppress fluorescent background in measured Raman spectra, which can be mainly categorized as experimental methods and computational method [7]. Experimental methods, including shift-excitation Raman difference spectroscopy [8], time-gated Raman spectroscopy [9], phase-resolved modulation Raman spectroscopy [10], *et al.*,

often require costly and sophisticated instrument. Although computational methods, such as polynomial fitting [11], [12], wavelet transform [13], [14], Fourier transform [15], derivative [16], and peak detection [17], [18], only rely on numerical calculation thus additional equipment is non-essential, such methods are limited by low fluorescence suppression efficiency or long computation time when a large number of Raman measurements need to be processed in a short time especially in Raman spectroscopic imaging. Therefore, a fast, efficient and cost-effective fluorescence background suppression method is desirable in the field of Raman spectroscopic imaging.

In this paper, an ultrafast suppression method based on the stepwise spectral reconstruction was demonstrated to overcome the limitations of the traditional computational methods in fluorescence suppression performance and computation efficiency. The proposed method was tested on spontaneous Raman measurements from phantoms and leukemia cells samples as well as the surface-enhanced Raman spectroscopy (SERS) measurements from blood serum samples. For comparison, four commonly used computational methods for fluorescence suppression, e.g. polynomial fitting, wavelet transform, Fourier transform, and peak detection, was tested on the same dataset. With the method of polynomial fitting as the golden standard, the results from the proposed method are closest to the reference, and the computation time is the shortest among all the above methods. Therefore, the ultrafast fluorescence suppression method based on the stepwise spectral reconstruction not only significantly improves fluorescence suppression performance but also shorten the computation time significantly, which is expected to be useful in Raman spectroscopic imaging.

II. MATERIALS AND METHODS

A. RAMAN SPECTRA MEASUREMENTS

Spontaneous Raman spectra measurements were taken from phantoms and leukemia cells, while SERS measurements were taken from blood serum samples.

1) PHANTOM

25 agar phantoms were made from the mixture of potassium formate (294454, Sigma-Aldrich, US) and urea (V3171, Promega corporation, US), in which the concentration for both potassium formate and urea included 0.25 M, 0.5 M, 1 M, 1.5 M, and 2 M. The spontaneous Raman spectra were measured by a micro-Raman system (innoRam-785S, B&W TEK, US) with 785nm laser excitation and the exposure time was 10 s accumulated with 30 times. The Raman measurements were taken from 600 cm^{-1} to 1800 cm^{-1} and the spectral resolution was 4cm^{-1}.

2) LEUKEMIA CELL

30 spontaneous Raman spectra were collected from live, apoptotic and necrotic leukemia cells under a confocal Raman microscope (inVia, Renishaw, UK), in which the number of cells in each group is 10. The excitation wavelength was 785 nm and the exposure time was 10 s accumulated with 6 times. The Raman measurements were taken from 600 cm^{-1} to 1800 cm^{-1} and the spectral resolution is 2cm^{-1}.

TABLE 1. Parameters of the fluorescence background methods and the ranges of parameters.

Method	Parameter	Parameter range
Polynomial fitting	Order	5-th
Wavelet transform	Wavelet basis	db1, db2, …, db25 sym2, sym3, …, sym8, coif1, coif2, …, coif5, bior1.3, bior2.2, bior2.6, bior3.1, bior3.5, bior3.9, bior5.5
	Decomposition number	2, 3, …, 15
	Threshold	Sort threshold: 0, 1000, …, 4000000 or Hard threshold: 0, 1000, …, 4000000
Fourier transform	Cut-off frequency	0, 0.1, …, 20
Peak detection	Smooth window size	2, 3, …, 100
	Peak elimination window size	2, 3, …, number of wavenumbers
Stepwise spectral reconstruction	Number of non-negative PCs based filters	2, 3, …, 15

3) BLOOD SERUM SAMPLE

50 SERS spectra were measured from blood serum samples of 50 nasopharyngeal cancer patients in Fujian Tumor Hospital in Fuzhou, China, in which the measurements were taken by a confocal Raman microscope (inVia, Renishaw, UK). The excitation wavelength was 785 nm and the exposure time was 10 s. The Raman measurements were taken from 600 cm^{-1} to 1800 cm^{-1} and the spectral resolution is 2 cm^{-1}.

B. DATA PROCESSING

All the measured Raman spectra were first preprocessed by sequential five-point smoothing in order to reduce the shot noise, which is named as de-noised Raman spectra in the following paragraphs, before the Raman spectra were further processed by the following fluorescence suppression algorithms. The methods used in this study and their corresponding parameter ranges are shown in Table 1, in which the polynomial fitting method serves as the gold standard during the evaluation of the fluorescence suppression efficiency in this study. The relative root mean square error (RMSE) [19] is used as the metric in the evaluation. All fluorescence background removal methods, including polynomial fitting, wavelet transform, Fourier transform, peak detection and stepwise spectral reconstruction were coded and run in Matlab (MATLAB R2012b, MathWorks, Natick, MA, USA).

1) POLYNOMIAL FITTING

The Raman spectra generally consist of Raman peaks and noise superimposed on fluorescence background, in which the fluorescence background varies slower with wavelength compared with the Raman spectrum. Thus, the polynomial model can be used to represent a wide class of fluorescence backgrounds. In this study, the fluorescence background is estimated by fitting the spectrum to a 5-th order polynomial in the least square sense and then subtracted from the de-noised Raman spectrum, in which the 5-th order polynomial fitting was iteratively performed to find the best fit curve with the intensity value not greater than that of the original Raman spectrum at every wavelength. More details about the proposed polynomial fitting method can be found in the literature [12].

2) WAVELET TRANSFORM

Wavelet transform is used to decompose the de-noised Raman spectrum into individual frequency components using different wavelet bases, and then restore the pure Raman signal after removing useless frequency components. In general, fluorescence background consists of slowly changes thus contains mainly low frequency components, while the Raman spectrum comprises sharp peaks carrying much higher frequency components. Thus, by removing those low-frequency components corresponding to the fluorescence background, the pure Raman signal can be extracted. The parameters of wavelet transform, e.g. the wavelet bases, decomposition number, and threshold as shown in Table 1, were optimized by exploring all possible combinations of different parameters.

3) FOURIER TRANSFORM

Fourier transform is used to represent the original signal in the frequency domain, in which components of high and low frequencies correspond to sharp and slow changes in the original signal, respectively. Similar to the earlier description, fluorescence background consists of slowly changes thus contains mainly low frequency components, while the Raman spectrum comprises sharp peaks carrying much higher frequency components. Thus, the fluorescence background can be removed by applying a high-pass filter with a proper cut-off frequency to the measured spectrum. In this study, the cut-off frequency was optimized in the range of 0 to 20, where the step size was 0.1.

4) PEAK DETECTION

Since the fluorescence background varies slower than the Raman spectrum, it can be estimated from a measured spectrum by eliminating significant peaks with high-frequency components. Thereafter, the estimated fluorescence background can be subsequently removed by simple subtraction from the original Raman spectrum. In this study, the peaks were inspected according to the smoothed derivative of a given spectrum, in which the maximum value of the peak occurs when the sign of the derivative changes from positive to negative and the boundary of the peak can be found at the adjacent zero positions of the derivative. More specifically, the smoothed derivative is obtained by smoothing with a window size varying from 2 to 100 and subsequent smoothing with a peak elimination window size varying from 2 to the number of wavenumber to remove sharp Raman peaks. After cropping the corresponding peak area, the fluorescence background was estimated by applying a modified linear interpolation, in which interpolated values were calculated by integrating the background's derivative in the peak region and the background can be obtained by assembling interpolated values for all peak regions together with untouched segments. Thereafter, the fluorescence background was removed by simple subtraction from the de-noised Raman spectrum. More details about the peak detection based fluorescence background suppression method can be found in the literature [17].

5) STEPWISE SPECTRAL RECONSTRUCTION

The stepwise spectral reconstruction method is developed for fast Raman spectroscopic imaging and it can reconstruct the pure Raman spectrum rapidly from a few narrow-band measurements, in which the narrow-band measurements are acquired in the presence of fluorescence background after the emitted light from a sample passes through a few selected filters one at a time. Thus, this method naturally possesses significant potential in fluorescence background removal.

The schematic of the stepwise spectral reconstruction method is shown in Figure 1. The stepwise spectral reconstruction is a supervised learning method in nature, thus it is necessary to establish a calibration dataset to train the model for fluorescence suppression. The calibration data set in this method include original Raman spectra, pure Raman spectra after fluorescence background removal, fluorescence background spectra and their corresponding narrow-band measurements, whereas the test data set include only original Raman spectra in the presence of fluorescence background. In this study, the narrow-band measurements N are defined as the inner product of the transmittance spectra of the given filters F and spectra S. Non-negative principal components (PCs) based filters [20] generated from the corresponding denoised Raman spectra, were used to generate the narrow-band measurements in this study. The transmittance spectra of these non-negative PCs based filters were derived from the principal component analysis (PCA) of Raman spectra measured from representative target samples, thus the resulting narrow-band measurements can benefit from the optimal compression properties of the PCA scheme. The number of PCs based filters was optimized in a range of 2 to 15.

Wiener estimation [20], [21] was used to train the model for fluorescence suppression. The procedure of Wiener estimation consists of two stages, i.e. the calibration stage and test stage. In the calibration stage, the Wiener matrix is constructed using narrow-band measurements N_c and spectra S in the calibration data set according to (1), in which the relation

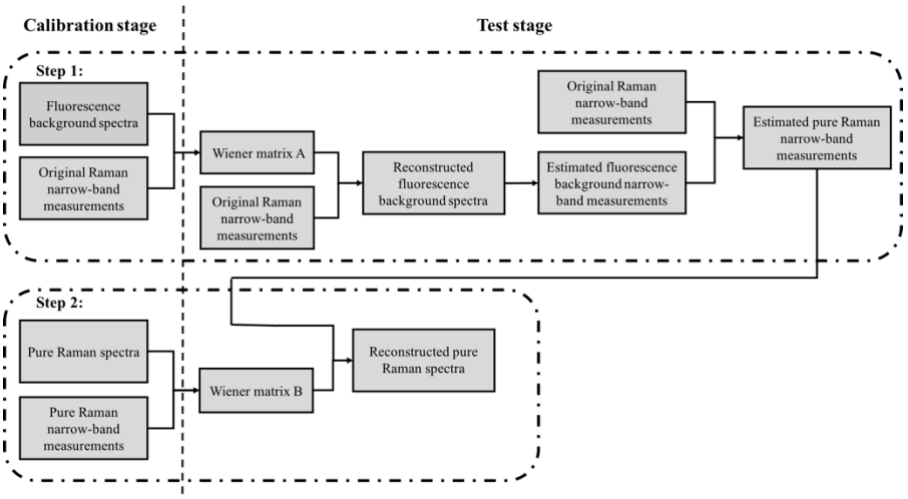

FIGURE 1. Schematic of the stepwise spectral reconstruction.

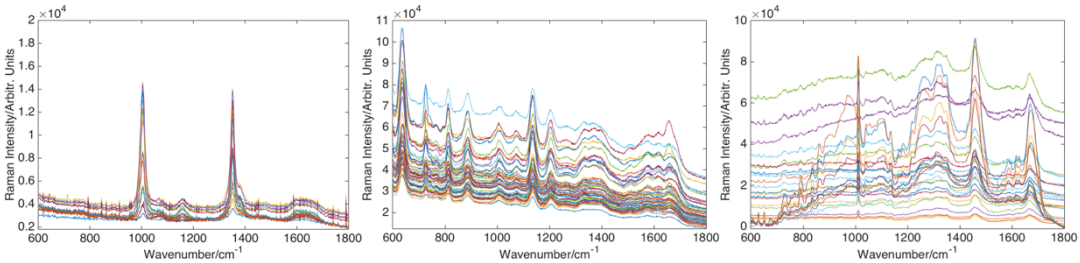

FIGURE 2. Original Raman spectra before fluorescence suppression: (a) spontaneous Raman spectra from phantoms, (b) SERS spectra from blood serum samples, and (c) spontaneous Raman spectra from leukemia cells.

between the narrow-band measurements N_c and spectra S is built. Wiener matrix A is created to relate fluorescence background spectra to the original Raman narrow-band measurements, and Wiener matrix B is created to relate pure Raman spectra to pure Raman narrow-band measurements.

$$W = \mathrm{E}\left(SN_c^{\mathrm{T}}\right)\left[\mathrm{E}\left(N_cN_c^{\mathrm{T}}\right)\right]^{-1} \tag{1}$$

where E () denotes the ensemble average, the superscript "T" denotes matrix transpose and the superscript "-1" denotes matrix inverse.

In the test stage, the Wiener matrix W is applied to narrow-band measurements N_t from the test dataset to reconstruct the corresponding spectrum R according to (2).

$$R = WN_t \tag{2}$$

The stepwise spectral reconstruction method performs spectral reconstruction in two steps in both the calibration stage and the test stage. This method first reconstructs the fluorescence background spectrum from the original Raman narrow-band measurements by Wiener estimation and then the pure Raman narrow-band measurements can be estimated by subtracting the estimated fluorescence background narrow-band measurements from the original Raman narrow-band measurements. Thereafter, the pure Raman spectrum is reconstructed from the estimated pure Raman narrow-band measurements by Wiener estimation. Since the calibration data set is required by such a method, a leave-one-out method [22] is used for cross validation to fully utilize each sample in an unbiased manner. More details about stepwise spectral reconstruction can be found in [23].

III. RESULTS

The original spontaneous Raman spectra from phantoms and leukemia cells as well as the original SERS spectra from blood serum samples are shown in Figure 2, in which Raman spectra from phantoms, blood serum samples and leukemia cells represent the cases of low fluorescence background, high fluorescence background, and moderate fluorescent background, respectively.

In our study, the same set of reference spectra was used for comparison across all methods being tested including our method and four other commonly used methods. Such comparison was made for Raman spectra from different types of samples in Figures 3 through 5 for comprehensive evaluation. The mean relative RMSE is calculated between the results from corresponding fluorescence background removal

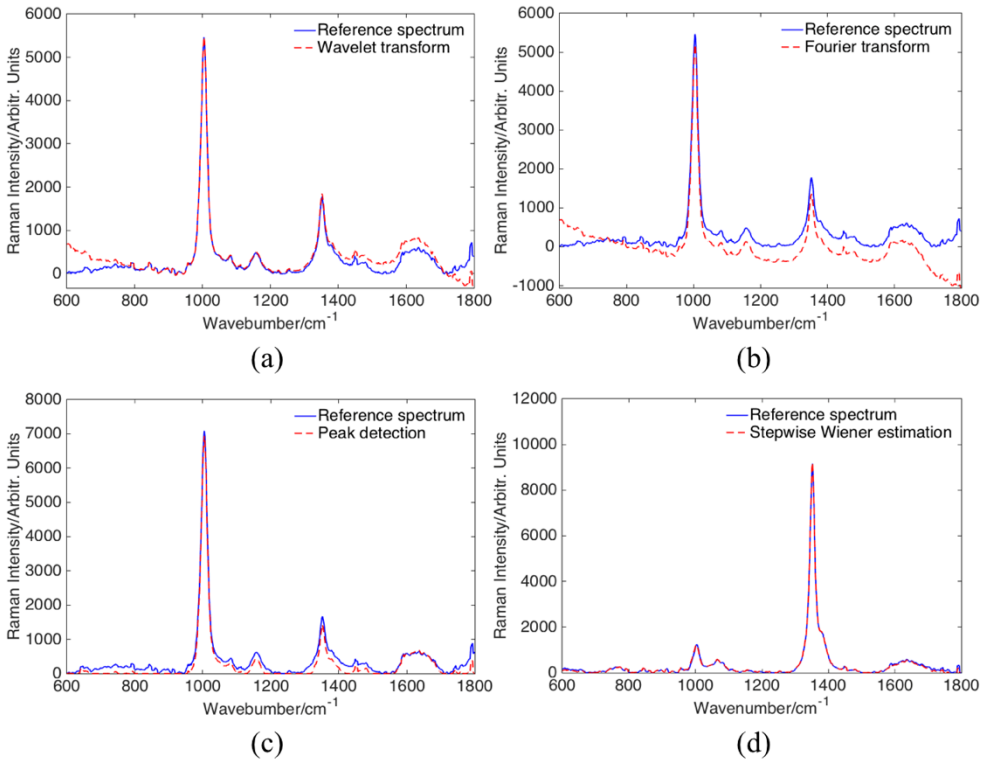

FIGURE 3. Comparison of the reference Raman spectrum of phantoms obtained using the 5th-order polynomial fitting and the corresponding Raman spectra extracted using the methods of wavelet transform, Fourier transform, peak detection, and the stepwise spectral reconstruction in the typical case, in which the relative RMSE is to the mean value.

method and standard method, i.e. the 5-th order polynomial fitting, and was used as the criterion to evaluate the fluorescence suppression efficiency. Table 2 shows comparison in the mean relative RMSE of Raman spectra after the fluorescence background removal using the methods of wavelet transform, Fourier transform, peak detection, and stepwise spectral reconstruction. According to the results in Table 2, the stepwise spectral reconstruction shows significant improvement compared with other fluorescence background removal methods in all respects. In order to compare each method in an unbiased manner, we chose one of the reconstructed spectra, whose relative RMSE is closest to the mean relative RMSE for the entire set, to represent the typical result of each method in Figures 3, 4 and 5. Although the typical result of each method may correspond to a different reference spectrum, it represented the overall performance of each method in fluorescence suppression efficiency.

For phantoms, all the configurations for each method were optimized to achieve the smallest mean relative RMSE. The result of wavelet transform is optimal when the wavelet basis is 'db5' with a decomposition number of 11 and a soft threshold of 220000. The result of Fourier transform is optimized when the cut-off frequency is 1.1. The result of peak detection is optimal when the smoothing window size is 7 and the peak elimination window size is 339. The result of the stepwise spectral reconstruction is optimal when the number of filters

TABLE 2. Comparison in the mean relative RMSE of Raman spectra after the fluorescence background is removed by different fluorescence background removal methods.

	Wavelet transform	Fourier transform	Peak detection	Stepwise spectral reconstruction
Phantom	0.0349	0.0840	0.0221	0.0045
Leukemia cell	0.2063	0.2924	0.0694	0.0184
Blood serum sample	0.1055	0.2095	0.0403	0.0111

is 4. According to Table 2, the mean relative RMSE for stepwise spectral reconstruction is 12.9%, 5.4%, and 20.4% of those for the wavelet transform, Fourier transform, and peak detection, respectively. Figure 3 shows the comparison of the reference Raman spectrum obtained with the 5th-order polynomial fitting and the corresponding Raman spectra extracted using the methods of wavelet transform, Fourier transform, peak detection and stepwise spectral reconstruction in the typical case, in which the relative RMSE is close to the corresponding mean value. The relative RMSEs in Figure 3 are 0.0354, 0.0837, 0.0219, and 0.0041 for wavelet transform,

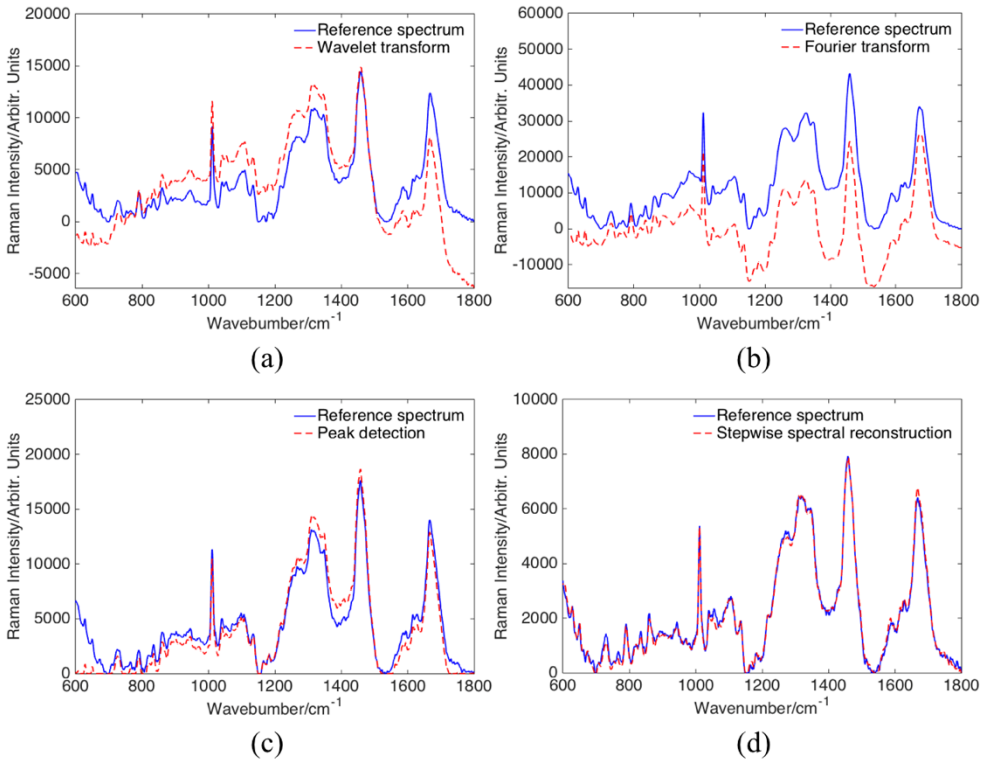

FIGURE 4. Comparison of the reference Raman spectrum of leukemia cells obtained using the 5th-order polynomial fitting and the corresponding Raman spectra extracted using the methods of wavelet transform, Fourier transform, peak detection, and the stepwise spectral reconstruction in the typical case, in which the relative RMSE is to the mean value.

Fourier transform, peak detection, and the stepwise spectral reconstruction, respectively.

For leukemia cells, the result of wavelet transform is optimized when the wavelet basis is 'db20' with a decomposition number of 11 and a soft threshold of 3000000. The result of Fourier transform is optimized when the cut-off frequency is 2.2. The result of peak detection is optimized when the smoothing window size is 39 and the peak elimination window size is 949. The result of the stepwise spectral reconstruction is optimized when the number of filters is 11. According to Table 2, the mean relative RMSE for the stepwise spectral reconstruction is 8.9%, 6.3%, and 26.5% of those for wavelet transform, Fourier transform, and peak detection, respectively. Figure 4 shows the comparison of the reference Raman spectrum obtained using the 5-th order polynomial fitting and the corresponding Raman spectrum extracted using the methods of wavelet transform, Fourier transform, peak detection, and stepwise spectral reconstruction in the typical case, in which the relative RMSE is close to the corresponding mean value. The relative RMSEs in Figure 4 are 0.2038, 0.2934, 0.0693, and 0.0179 for the wavelet transform, Fourier transform, peak detection, and stepwise spectral reconstruction, respectively.

For the SERS spectra of blood serum samples, the result of wavelet transform is optimized when the wavelet basis is 'db3' with a decomposition number of 11 and a soft threshold of 3694000. The result of Fourier transform is optimized when the cut-off frequency is 10.8. The result of peak detection is optimized when the smoothing window size is 47 and the peak elimination window size is 207. The stepwise spectral reconstruction is optimized when the number of filters is 11. According to Table 2, the mean relative RMSE for the stepwise spectral reconstruction is 10.5%, 5.3%, 5.4%, and 27.5% of those for the methods of wavelet transform, Fourier transform, and peak detection, respectively. Figure 5 shows the comparison of the reference Raman spectrum obtained using the 5-th order polynomial fitting and the corresponding Raman spectrum extracted using the methods of wavelet transform, Fourier transform, peak detection, and stepwise spectral reconstruction in the typical case, in which the relative RMSE is close to the corresponding mean value. The relative RMSEs in Figure 5 are 0.1059, 0.2093, 0.0402, and 0.0110 for wavelet transform, Fourier transform, peak detection, and stepwise spectral reconstruction, respectively.

IV. DISCUSSIONS

According to the above results, the stepwise spectral reconstruction always shows the best performance, while the Fourier transform method always shows the worst performance in terms of agreement with the reference Raman spectra after fluorescence background removal. In addition, the fluorescence suppression performance degrades as

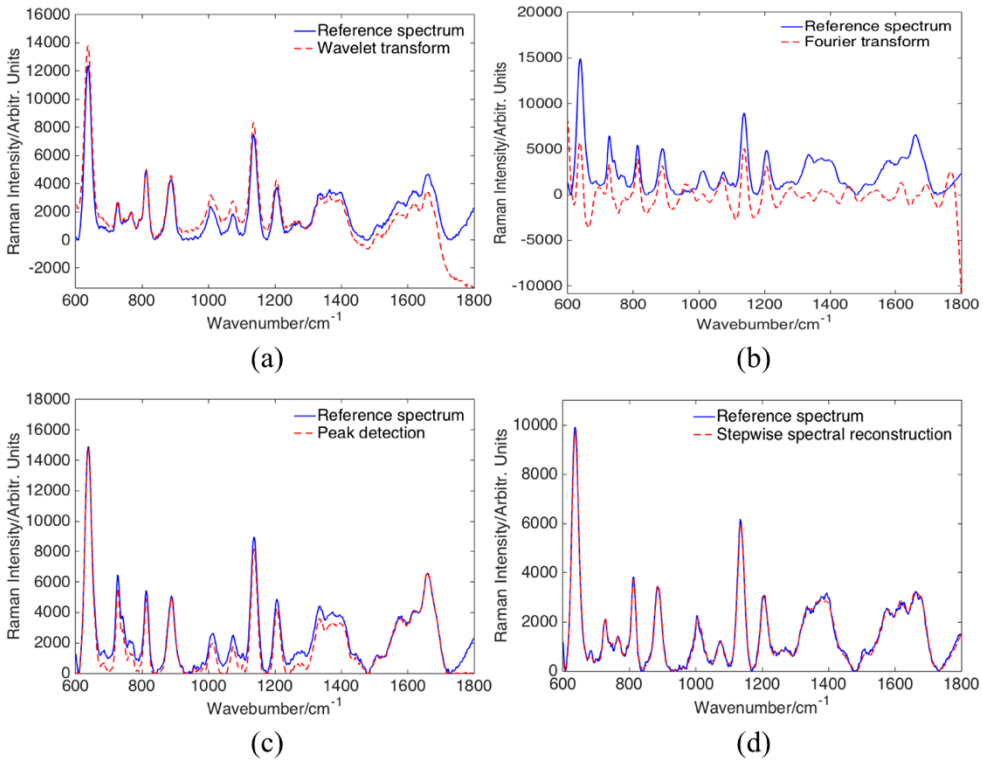

FIGURE 5. **Comparison of the reference SERS spectrum of blood serum samples obtained using the 5th-order polynomial fitting and the corresponding Raman spectra extracted using the methods of wavelet transform, Fourier transform, peak detection, and the stepwise spectral reconstruction in the typical case, in which the relative RMSE is to the mean value.**

fluorescence background increases. For example, the fluorescence suppression results of phantom spectra, which contain the lowest background, are always the best; while those of the leukemia cell spectra are always the lowest. According to Figures 3(d), 4(d), and 5(d), the agreement in the peak locations between the reference Raman spectra and the Raman spectra after fluorescence background removal using the stepwise spectral reconstruction method is excellent and the spectral shape information is mostly preserved. We believe that the following reason causes the proposed method to outperform other common methods in this study. Since the proposed spectral reconstruction method is a supervised learning method in nature, the prior knowledge about the fluorescence background and pure Raman signal in the calibration data set helps extract fluorescence background and reconstruct pure Raman spectra in the first and second step of stepwise spectral reconstruction. Such a unique advantage is unavailable in other methods that are essentially unsupervised. Furthermore, since this method requires a calibration dataset, the performance largely depends on the quality of reference Raman spectra in the calibration dataset. In this study, the 5-th order polynomial fitting was used for fluorescence background removal to generate reference spectra in the calibration stage. However, the fluorescence suppression performance of 5-th order polynomial fitting may not be optimal in some cases. Thus, it is anticipated that the performance of the stepwise spectral reconstruction can be better or worse if a set of reference Raman spectra with fluorescence background suppressed to a different extent is used in the calibration dataset. It is worth noting that even a calibration dataset is required in the proposed method, this method can be useful in a large number of biomedical applications in which the speed of data processing is critical and a calibration data set is available. The peak detection method can preserve most peak locations and spectral shape. However, peak intensities are occasionally inaccurate and some small peaks are missing. This might be the consequence of excessive smoothing during peak localization. Although the wavelet transform and Fourier transform methods can preserve the locations of many peaks, partial fluorescence background is retained and some Raman peaks and their intensity values are not recovered well, which are especially true for the Fourier transform method. This might be due to the frequency overlap between the Raman peaks and some uneven fluorescence background.

The computation efficiency was evaluated for performing fluorescence background suppression of 90,000 leukemia cells' Raman spectra for all above methods. Those methods were coded and tested in a computer with 3.3 GHz Intel(R) Core(TM) i5-4590 CPU, 4G RAM and Windows 7 operating system. Each method was tested for 5 times and the computation time was averaged to find the mean value as shown

TABLE 3. Computation time taken to remove fluorescence background in 90,000 spontaneous Raman spectra using the methods of polynomial fitting, wavelet transform, Fourier transform, peak detection and stepwise spectral reconstruction.

	Polynomial fitting	Wavelet transform	Fourier transform	Peak detection	Stepwise spectral reconstruction
Time(s)	9608.208	615.3421	10.8812	518.5507	0.7667

in Table 3. According to Table 3, the stepwise spectral reconstruction method is the fastest one, for which the computation time is 0.008%, 0.125%, 7.046%, and 0.148% of the methods of polynomial fitting, wavelet transform, Fourier transform, peak detection, respectively. The reason for this method to be computationally efficient is that the Wiener matrix from the calibration dataset can be calculated beforehand and the final outcome can be derived with matrix multiplication for just a few times, whereas others require heavy computation, e.g. polynomial fitting, wavelet transform, Fourier transform or complex operation. Such a fast method is important in Raman spectroscopic imaging in which fluorescence suppression needs to be conducted for a large number of pixels at the same time.

V. CONCLUSION

In this study, a fast fluorescence suppression method based on the strategy of stepwise spectral reconstruction was proposed to overcome the low computation efficiency of traditional computational methods. The proposed method was evaluated on Raman spectra measured from phantoms and cells as well as surfaced enhanced Raman spectra from blood serum samples and compared with several commonly used fluorescence suppression methods. The results show that our method yields clean Raman spectra closest to the reference results generated by polynomial fitting while several orders of magnitude faster than others. Therefore, the proposed fast fluorescence suppression method is promising in Raman spectroscopic imaging or related applications in which high computation efficiency is critical and a calibration dataset is available.

REFERENCES

[1] Y. H. Ong, M. Lim, and Q. Liu, "Comparison of principal component analysis and biochemical component analysis in Raman spectroscopy for the discrimination of apoptosis and necrosis in K562 leukemia cells," *Opt. Express*, vol. 20, no. 22, pp. 22158–22171, Sep. 2012.

[2] S. Chen, Y. H. Ong, and Q. Liu, "A method to create a universal calibration dataset for Raman reconstruction based on Wiener estimation," *IEEE. J. Sel. Topics Quantum Electron.*, vol. 22, no. 3, May/Jun. 2016, Art. no. 6800407.

[3] S. Feng, W. Wang, I. T. Tai, G. Chen, R. Chen, and H. Zeng, "Label-free surface-enhanced Raman spectroscopy for detection of colorectal cancer and precursor lesions using blood plasma," *Biomed. Opt. Express*, vol. 6, no. 9, pp. 3494–3502, Sep. 2015.

[4] T. Mu *et al.*, "High-sensitive smartphone-based Raman system based on cloud network architecture," *IEEE. J. Sel. Topics Quantum Electron.*, vol. 25, no. 1, Jan/Feb. 2019, Art. no. 7200306.

[5] E. B. Hanlon *et al.*, "Prospects for *in vivo* Raman spectroscopy," *Phys. Med. Biol.*, vol. 45, no. 2, p. R1, Mar. 2000.

[6] J. Kostamovaara, J. Tenhunen, M. Kögler, I. Nissinen, J. Nissinen, and P. Keränen, "Fluorescence suppression in Raman spectroscopy using a time-gated CMOS SPAD," *Opt. Express*, vol. 21, no. 25, pp. 31632–31645, Dec. 2013.

[7] D. Wei, S. Chen, and Q. Liu, "Review of fluorescence suppression techniques in Raman spectroscopy," *Appl. Spectrosc. Rev.*, vol. 50, no. 5, pp. 387–406, 2016.

[8] M. T. Gebrekidan, C. Knipfer, F. Stelzle, J. Popp, S. Will, and A. Braeuer, "A shifted-excitation Raman difference spectroscopy (SERDS) evaluation strategy for the efficient isolation of Raman spectra from extreme fluorescence interference," *J. Raman Spectrosc.*, vol. 47, no. 2, pp. 198–209, Feb. 2016.

[9] T. Rojalin *et al.*, "Fluorescence-suppressed time-resolved Raman spectroscopy of pharmaceuticals using complementary metal-oxide semiconductor (CMOS) single-photon avalanche diode (SPAD) detector," *Anal. Bioanal. Chem.*, vol. 408, no. 3, pp. 761–774, Jan. 2016.

[10] A. Z. Genack, "Fluorescence suppression by phase-resolved modulation Raman scattering," *Anal. Chem.*, vol. 56, no. 14, pp. 2957–2960, 1984.

[11] V. Mazet, C. Carteret, D. Brie, J. Idier, and B. Humbert, "Background removal from spectra by designing and minimising a non-quadratic cost function," *Chemometrics Intell. Lab. Syst.*, vol. 76, no. 2, pp. 121–133, Apr. 2005.

[12] Z. Huang, A. Mcwilliams, H. Lui, D. I. Mclean, S. Lam, and H. Zeng, "Near-infrared Raman spectroscopy for optical diagnosis of lung cancer," *Int. J. Cancer*, vol. 107, no. 6, pp. 1047–1052, 2003.

[13] C. M. Galloway, E. C. Le Ru, and P. G. Etchegoin, "An iterative algorithm for background removal in spectroscopy by wavelet transforms," *Appl. Spectrosc.*, vol. 63, no. 12, pp. 1370–1376, Dec. 2009.

[14] P. M. Ramos and I. Ruisánchez, "Noise and background removal in Raman spectra of ancient pigments using wavelet transform," *J. Raman. Spectrosc*, vol. 36, no. 9, pp. 848–856, Sep. 2005.

[15] C. A. Lieber and A. Mahadevan-Jansen, "Automated method for subtraction of fluorescence from biological Raman spectra," *Appl. Spectrosc.*, vol. 57, no. 11, pp. 1363–1367, Nov. 2003.

[16] M. N. Leger and A. G. Ryder, "Comparison of derivative preprocessing and automated polynomial baseline correction method for classification and quantification of narcotics in solid mixtures," *Appl. Spectrosc.*, vol. 60, no. 2, pp. 182–193, Feb. 2006.

[17] S.-J. Baek, A. Park, J. Kim, A. Shen, and J. Hu, "A simple background elimination method for Raman spectra," *Chemometrics Intell. Lab. Syst.*, vol. 98, no. 1, pp. 24–30, Aug. 2009.

[18] Z.-M. Zhang *et al.*, "An intelligent background-correction algorithm for highly fluorescent samples in Raman spectroscopy," *J. Raman Spectrosc.*, vol. 41, no. 6, pp. 659–669, Jun. 2010.

[19] S. Chen, X. Lin, C. Yuen, S. Padmanabhan, R. W. Beuerman, and Q. Liu, "Recovery of Raman spectra with low signal-to-noise ratio using Wiener estimation," *Opt. Express*, vol. 22, no. 10, pp. 12101–12114, May 2014.

[20] S. Chen, Y. H. Ong, X. Lin, and Q. Liu, "Optimization of advanced Wiener estimation methods for Raman reconstruction from narrow-band measurements in the presence of fluorescence background," *Biomed. Opt. Express*, vol. 6, no. 7, pp. 2633–2648, Jul. 2015.

[21] S. Chen, Y. H. Ong, and Q. Liu, "Fast reconstruction of Raman spectra from narrow-band measurements based on Wiener estimation," *J. Raman Spectrosc.*, vol. 44, no. 6, pp. 875–881, Jun. 2013.

[22] J. S. U. Hjorth, *Computer Intensive Statistical Methods: Validation, Model Selection, and Bootstrap*. New York, NY, USA: CRC Press, 1993, pp. 27–28.

[23] S. Chen, G. Wang, X. Cui, and Q. Liu, "Stepwise method based on Wiener estimation for spectral reconstruction in spectroscopic Raman imaging," *Opt. Express*, vol. 25, no. 2, pp. 1005–1018, Jan. 2017.

SHUO CHEN received the bachelor's degree from Shanghai Jiao Tong University, China, and the master's degree from Heidelberg University, Germany, and the Ph.D. degree from the School of Chemical and Biomedical Engineering, Nanyang Technological University, Singapore. He is currently an Associate Professor with the Sino-Dutch Biomedical and Information Engineering School, Northeastern University, China. His research interest is focused on fast spectroscopic imaging in biomedical applications.

LINGMIN KONG received the bachelor's degree from the Taiyuan University of Technology, China. He is currently pursuing the master's degree with the Sino-Dutch Biomedical and Information Engineering School, Northeastern University, China. His research interest is focused on fast spectroscopic imaging in biomedical applications.

WENBIN XU received the Ph.D. degree in optical engineering from the University of Chinese Academy of Sciences. He is currently a Senior Engineer with the Science and Technology on Optical Radiation Laboratory, Beijing Institute of Environmental Features. His research interest focuses on infrared spectroscopy, spectral data processing in industrial applications.

XIAOYU CUI received the bachelor's degree from the Shenyang University of Technology, China, and the master's and Ph.D. degrees in biomedical engineering from Northeastern University, China. He is currently an Associate Professor with the Sino-Dutch Biomedical and Information Engineering School, Northeastern University. His research interests are focused on optical imaging and machine learning in biomedical applications.

QUAN LIU received the bachelor's degree in electrical engineering from Xidian University, Xi'an, China, the master's degree in electrical engineering from the Graduate School, University of Science and Technology of China, Beijing, China, and the Ph.D. degree in biomedical engineering from the University of Wisconsin-Madison, Madison, WI, USA. He is currently an Associate Professor with the School of Chemical and Biomedical Engineering, Nanyang Technological University, Singapore. He has published more than 50 journal papers. He held 15 U.S. patents/applications in the field of biomedical optics. His current research interests include fast spectroscopic optical imaging, depth sensitive optical spectroscopy, and surface enhanced Raman spectroscopy for malaria diagnosis. He is a Senior Member of the SPIE and OSA.